

Water Resources Research

RESEARCH ARTICLE

10.1029/2018WR023592

Key Points:

- Biotransformation of pharmaceuticals takes place in small to medium streams
- OECD 308 tests underestimate pharmaceutical biotransformation rates yet overestimate total degradation in the Rhine basin
- Assessment of pharmaceutical persistence from measured river fluxes is conditional on precise emission and removal data

Supporting Information:

- Supporting Information S1

Correspondence to:

M. Honti,
mark.honti@gmail.com

Citation:

Honti M., Bischoff, F., Moser, A., Stamm, C., Baranya, S., & Fenner, K. (2018). Relating degradation of pharmaceutical active ingredients in a stream network to degradation in water-sediment simulation tests. *Water Resources Research*, 54, 9207–9223. <https://doi.org/10.1029/2018WR023592>

Received 29 JUN 2018

Accepted 29 OCT 2018

Accepted article online 5 NOV 2018

Published online 22 NOV 2018

Relating Degradation of Pharmaceutical Active Ingredients in a Stream Network to Degradation in Water-Sediment Simulation Tests

Mark Honti¹ , Fabian Bischoff², Andreas Moser² , Christian Stamm² , Sándor Baranya³ , and Kathrin Fenner^{2,4} 

¹MTA-BME Water Research Group, Hungarian Academy of Sciences, Budapest, Hungary, ²Department of Environmental Chemistry, EAWAG Swiss Federal Institute of Aquatic Science and Technology, Dübendorf, Switzerland, ³Department of Hydraulic and Water Resources Engineering, Budapest University of Technology and Economics, Budapest, Hungary, ⁴Chemistry Department, University of Zürich, Zürich, Switzerland

Abstract Many pharmaceuticals inevitably end up in surface waters, exerting unwanted biological activity in nontarget organisms. This effect is confined by the compound's environmental persistence. Regulatory laboratory simulation tests are used in persistence assessment and exposure modeling. While doubt has been expressed about the usefulness of laboratory-derived persistence indicators under field conditions, these remain the only inputs for chemical fate models due to difficulties of measuring persistence in situ, especially at large scales. To improve understanding about relationships between laboratory experiments and the environmental fate in streams, we developed a mathematical model of biodegradation in stream networks and combined it with in-stream monitoring data to (i) test if persistence could be evaluated from field data, (ii) check if persistence extracted from laboratory tests applied in the field, and (iii) locate hot spots of biodegradation in a large river basin. The model describes partitioning, and particle settling and resuspension, and is structurally compatible with those applied for evaluating laboratory simulation tests. Application to the Rhine river basin suggests that biotransformation rate constants extracted from laboratory tests underestimate those in the field, yet the percentage of biotransformation in the Rhine basin is less than in the laboratory tests due effective biotransformation being limited to small- and medium-sized streams. In conclusion, our data show that biotransformation rates can accurately be predicted if (i) monitoring is performed across a wide range in stream order and (ii) precise estimates for consumption and removal rates at wastewater treatment plants are known.

1. Introduction

The production, use, and disposal of plant protection products, human, and veterinary pharmaceuticals, biocides, and industrial chemicals inevitably lead to the pollution of surface water bodies due to direct use in the environment, accidental spills, or incomplete removal during wastewater treatment. Since most of these substances intentionally exhibit biological activity, they bear the potential to harm aquatic ecosystems. Although continuous emissions can make chemicals seem pseudopersistent, the actual levels of their pollution and its duration after emission has ceased are determined by (real) persistence, that is, how fast the pollutant is removed by biological and chemical degradation processes (Boethling et al., 2009). For surface water systems, the most important transformation processes determining persistence include chemical hydrolysis, direct and indirect phototransformation, and microbial biotransformation. The speed and extent of these transformation processes determine the persistence of chemicals and therefore play an important role in the regulatory risk assessment of chemicals. In regulatory frameworks, a compound's persistence is often assessed in laboratory-based test systems using a so-called tiered approach (i.e., if the compound fails to be degraded in the rather simple, yet stringent lower-tier tests, its degradation is studied in increasingly complex yet environmentally more realistic higher-tier test systems; cf. REACH [ECHA], Canadian Guideline for Determining Environmental Chemistry and Fate of Pesticides [Agriculture Canada, Environment Canada, and Department of Fisheries and Oceans 1987], EPA OPPTS Guidelines [U.S. EPA]).

The higher-tier test systems, also called simulation tests, are meant as closer representations of the real environment compared to biodegradability and hydrolysis tests, yet they exhibit superior reproducibility and

lower costs compared to tests carried out in the field. As a consequence, they form the backbone of regulatory assessment in cases when simpler tests cannot prove the lack of persistence in the environment, which, due to their rather complex chemical structure, is the case for most water-relevant organic micropollutants such as pesticides and pharmaceuticals. For the evaluation of the microbial biotransformation of chemicals in surface water systems, two Organisation for Economic Co-operation and Development (OECD) testing guidelines are relevant: the OECD 308 guideline (*Aerobic and Anaerobic Transformation in Aquatic Sediment Systems*), which targets transformation at the water-sediment interface, and the OECD 309 guideline (*Aerobic mineralization in surface water—Simulation biodegradation test*), which assesses transformation in the pelagic water body (with or without a certain amount of suspended sediment). Simulation tests have a double purpose: They should provide a standardized platform to get comparable information about the biotransformation of chemicals in freshwater systems for regulatory persistence assessment and to yield relevant environmental half-lives for exposure modeling.

The usage of simulation test results in exposure modeling presumes that persistence parameters and indicators are transferable to real catchments. However, parameter transfer from laboratory to the field has been shown to be challenging even for abiotic processes. Catchments typically show lower abiotic process rates than the targeted laboratory systems (Liu et al., 2013; Pačes, 1983; Swoboda-Colberg & Drever, 1993; Wen & Li, 2018), with different physical conditions and heterogeneity as main suspects for the systematic difference. The persistence of organic micropollutants is governed by biological processes on the top of abiotic conditions, suggesting a more complex relationship. However, the extrapolation of biotransformation rates from laboratory to the field has not been systematically addressed yet. This gap is of high regulatory relevance; therefore, we focus on the usefulness of laboratory-derived persistence indicators in exposure modeling inside a large river basin.

Since its introduction, various issues with OECD 308 have been reported and discussed (Davis et al., 2005; Ericson, 2007; Ericson et al., 2013; Radke & Maier, 2014). A main point of criticism was the concern about the relevance of the test conditions with regard to degradation in actual surface water bodies. OECD 308 is carried out in a dark and stagnant environment, where 2–3 cm of settled—and mostly anaerobic—sediment lies under a 6 to 9-cm-shallow water column. Due to the complete lack of mixing, there is no suspended sediment and mass transport is limited to molecular diffusion. The low water-sediment ratio, the shallow depth of the water column, and stagnant conditions were listed as atypical for most surface water bodies affected by pharmaceutical emissions. These issues do not preclude using these tests for the regulatory assessment of persistence, yet they question their relevance for field conditions.

The OECD 309 system is criticized for being (i) vaguely standardized due to the numerous allowed variants (pelagic/nonpelagic, light/dark) and (ii) a very expensive form of hydrolysis and sorption test due to the typically very low level of biotransformation observed in such systems—probably due to the low provision of organic matter and degrader biomass.

Scientific literature reports on other types of persistence experiments that seek to more closely mimic the situation in the natural environment, such as flumes (Kunkel & Radke, 2008; Li et al., 2015), limnocorrals (Liber et al., 1997; Solomon et al., 1985), and mass balance experiments in the field (Fono et al., 2006; Huntscha et al., 2008; Tixier et al., 2002, 2003), yet these have not penetrated into regulatory practice yet.

Criticism against simulation studies can be distilled into issues about system complexity and definition: On the one hand, a simulation test is too complex to interpret its results directly. Biotransformation usually interferes with phase transfer and formation of nonextractable residues so that the extraction of degradation half-lives requires inverse modeling (Honti & Fenner, 2015). On the other hand, the test systems are overly simplistic and too strictly standardized compared to the complexity and variability of the real environment. The majority of flowing waters with their complex sediment dynamics is represented well by neither the stirred-suspended nor the stagnant experimental types. While there is a scientific consensus that experimental persistence does not directly project into persistence in the environment, to this day we still lack methods that could relate half-lives in specific laboratory systems to half-lives in the field. Presumably, the wide spectrum of physical conditions in surface water systems suggests that such methods should rely on certain physics-independent indicators of persistence, which could then be related to the specific environmental conditions. Yet common experimental persistence indicators are all specific to the experimental system.

The k'_{bio} concept (Honti et al., 2016) disentangles biotransformation from phase transfer and bioavailability in OECD 308 and OECD 309 type test systems, which allows converting half-lives between different compartments and experimental types. However, the model of Honti et al. (2016) is limited to closed experimental systems and therefore is not suited to simulate behavior under field conditions.

Therefore, we extended this model to streams to allow for a direct comparison with monitoring results for pharmaceuticals along the river Rhine measured by Ruff et al. (2015) and to address the following research questions:

1. Can persistence of chemicals in a stream network be evaluated from field data?
2. Can experimental half-lives measured in the laboratory be used in the field?
3. Where along a stream network is biotransformation the most intense?

We present a new model that describes the biotransformation of pharmaceuticals in the riverine environment in analogy to the spiraling concept developed for nutrient cycling in streams (Ensign & Doyle, 2006; Newbold et al., 1981). Nutrients pass through various abiotic and biotic stages along their travel downstream, which can be conceptualized as an extension of the local nutrient cycle into a spatial spiral. Micropollutants undergo rather similar processes: The cycle of phase partitioning pathways taking place in closed simulation tests, such as the OECD 308 and 309, develops into a spiral in streams, which in turn leaves its imprint on the observable behavior of the pollutant in the field. We formulate a simple first-order model structure that contains phase partitioning and downstream transport in an integrated manner. It is assumed that emissions and flow are both permanent (continuous and constant), which is reasonable for pharmaceuticals. Loss processes other than biotransformation (phototransformation, hydrolysis, etc.) are not considered in the model, yet we show how they can be included.

The present study approaches modeling micropollutant biotransformation in stream networks from the regulatory side. This approach requires a coverable data demand to reduce the uncertainty of calibration, careful consideration of sediment dynamics to ensure a realistic description of partitioning, and a structural compatibility with models developed for OECD 308 systems (beyond taking the lab-derived half-lives) to facilitate parameter comparison between the laboratory systems and the field.

There are already models simulating the fate and transport of micropollutants in (European) stream networks, but none of them fulfills the above requirements completely. The GREAT-ER model (Feijtel et al., 1997; Koormann et al., 2006) determines predicted environmental concentration values in individual stream segments using a stochastic approach. GREAT-ER solves analytical versions of transport equations and uses seasonal scenarios instead of time dynamics. The STREAM-EU model (Lindim et al., 2016) simulates transport in all media, not only surface waters, combining high spatial resolution and time dynamics, resulting in a highly complex mathematical structure and a corresponding high data demand. The WATER model (Trapp & Matthies, 1998) describes in-stream transport, yet sediment dynamics are controlled by parameters unrelated to both hydraulic properties of the reach and sediment quality. The TOXRIV model (Trapp & Matthies, 1998) does not assume steady states and hence requires detailed hydraulic and water quality data. In summary, structural compatibility to OECD 308 is missing from all of the above models, partitioning is oversimplified in certain models, and some are just too complex compared to data availability in large catchments.

2. Methods

The new model is based on river reaches, where partitioning and transformation in an equilibrium state are described as functions of the physical properties of the reach and the physicochemical properties of the compound. The pollutant's behavior in an entire catchment is simulated by connecting multiple stream reaches following the topology of the stream network.

The Rhine catchment upstream of the Dutch-German border is presented as a case study. The stream network is built up from reaches, and basic physical properties were assigned based on the CCM2 river and catchment database (EU JRC, <http://ccm.jrc.ec.europa.eu/>). The model is calibrated for seven active pharmaceutical ingredients (APIs) using emission data from the CrossWater project (Ingold et al., 2018; Moser et al., 2018), estimated excretion and wastewater treatment plant (WWTP) removal data from Singer et al. (2016), and pharmaceutical flux measurements by Ruff et al. (2015). Model results are analyzed both in terms of parameter values and spatial distribution. Calibrated biotransformation parameters are compared to

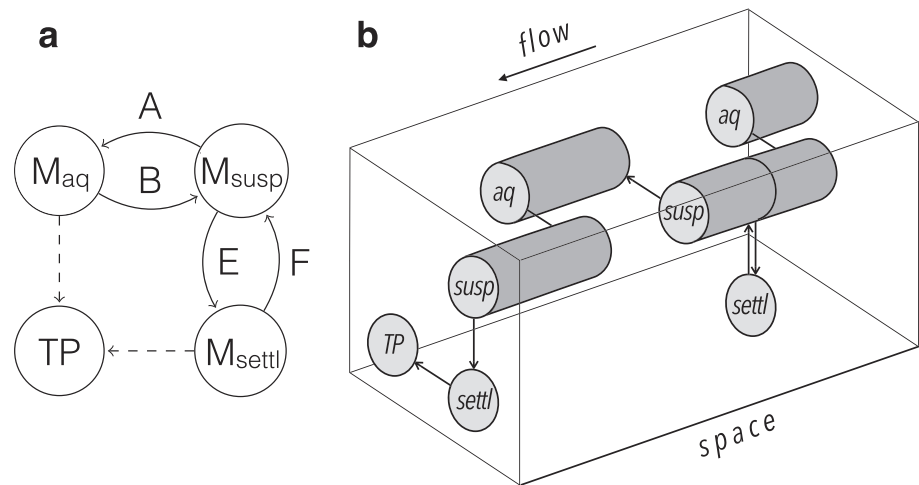


Figure 1. Partitioning and transformation pathways (a) and example for the flow-induced spiraling pattern in streams (b).

values obtained from regulatory studies. Calculated degradation of APIs in different parts of the stream network is analyzed to reveal potential hot spots of degradation.

Out of the seven APIs, four are kept anonymous and will be referred to here as API6, API8, API9, and API13, as their confidential OECD 308 experimental dossiers were kindly provided by the German Environment Agency (Fenner et al., 2016). Their coding here is not consecutive in order to keep the original codes of Fenner et al. (2016). The remaining three APIs lack associated experimental results; they are carbamazepine (CMZ), sitagliptin (SIG), and trimethoprim (TTP).

2.1. Partitioning and Transformation in a Stream Reach

We focus on the parent compound (the API). It is assumed that the total mass of the parent compound (M_{total}) is split between three different states: aqueous phase in water column (M_{aq}), sorbed to a suspended particle in water column (M_{susp}), or in the settled sediment (M_{settl}), including both aqueous state in porewater and being sorbed onto settled particles. Processes connecting the different partitioned states are sorption, desorption, settling, and resuspension (see Figure 1a).

We assume that sorbed fractions are not bioavailable; biotransformation from parent compound to transformation products of any kind can happen only from the aqueous phases in the water column and the sediment (e.g., from porewater; see Figure 1a). This does not contradict the fact that the majority of degrader biomass resides in biofilms covering resuspended or settled particles. It has been widely shown that the sorbed fraction is hardly or not at all bioavailable to microorganisms (section 26.4 in Schwarzenbach et al., 2016), and hence, the degrader biomass must mainly feed on the aqueous phase, whose renewal may be limited by the rate of desorption.

We furthermore assume a resuspension-settling equilibrium, which is reasonable for mean flow conditions. This means that both the settled active sediment layer and the suspended sediment stock are steady inside the reach. This obviously means that the model is invalid for conditions when this assumption is not met (e.g., under bed-moving floods or net deposition along the entire reach).

When all processes are first-order with rate constants denoted by A to F (Figure 1, A is the desorption rate constant, B is the sorption rate constant, E is the settling rate constant, and F is the resuspension rate constant), equilibrium partitioning can be expressed as $M_{aq}/M_{susp} = A/B$ and $M_{settl}/M_{susp} = E/F$ (see details in section S1 in the supporting information [SI]). Furthermore, $M_{aq} + M_{susp} + M_{settl} = M_{total}$, so $M_{susp}/M_{total} = (A/B + 1 + E/F)^{-1}$. The dimensionless ratios A/B and E/F derive from the properties of the stream reach and the API. A/B describes the sorption equilibrium between water and suspended sediment: $A/B = (K_d \cdot SSC)^{-1}$, where K_d is the sediment-water partitioning coefficient (m^3/kg), and SSC is the suspended sediment concentration (kg/m^3). Similarly, E/F characterizes the resuspension-settling equilibrium in the reach, $E/F = S (SSC \cdot Z_w)^{-1}$, where S is the resuspendable sediment stock in the active layer (kg/m^2) and Z_w is the water depth (m).

Transformation pathways are asymmetrical; they do not start from each state of the API and do not proceed at the same rates. They therefore slightly change the ratios between different API states, but this remains negligible when transformation rate constants are much smaller than $A - F$ (which is fulfilled for not readily degrading compounds, see section S1.1 in the SI).

In a flowing system, the partitioning cycle becomes a spiral, for example, partitioning is superimposed with longitudinal displacement (just as a spiral stems from superimposing rotation and longitudinal movement). The spiral for a single molecule develops in a random way. Even in steady flow, displacement is not uniform as states M_{aq} and M_{susp} get carried downstream, but M_{settl} remains still (Figure 1b). Propagation of the entire compound flux can be described by the mean of individual random spirals, where averaging smooths out randomness. The description of spiraling en masse requires expressing how partitioning affects mean downstream propagation (in terms of travel or residence time) and degradation kinetics at the system level. The first only depends on partitioning. The mean residence time of the parent compound in the control volume (τ^* [s]) relative to the mean water residence time (τ_w [s]), or retention, is simply

$$\frac{\tau^*}{\tau_w} = \frac{\frac{A}{B} + 1 + \frac{E}{F}}{1 + \frac{A}{B}} = 1 + \frac{\frac{S}{SSC \cdot Z_w}}{1 + \frac{1}{K_d \cdot SSC}}. \quad (1)$$

For the derivation of this equation please see section S1.1 in the SI. The A/B ratio is actually the aqueous-sorbed ratio of the API in the water column; E/F is the settled-resuspended mass ratio of the sediment. The $\frac{\tau^*}{\tau_w}$ dimensionless factor corrects the water residence time for the fraction of the compound that is sorbed to the settled sediment and therefore cannot move with the flow of water and suspended particles.

The description of system-level degradation needs a concept that links the degradation rate constants in the water and sediment compartments. The k'_{bio} concept introduced by Honti et al. (2016) does exactly this for compounds not subject to hydrolysis and photodegradation. The first-order compartment-level biotransformation rate constant is the product of the second-order k'_{bio} constant, the particulate organic carbon concentration as a proxy for degrader biomass, and the aqueous (bioavailable) fraction of the compound in the specific compartment (equations (S15) and (S19) in the SI). Utilizing this connection between the first-order compartment-level rate constants, one can express their ratio using the dimensionless properties of the system (for details see section S2 in the SI):

$$\frac{k_{sed}}{k_w} = \frac{\frac{A}{B} + 1}{\frac{A}{B} \frac{F}{E} \frac{Z_a}{Z_w} + 1} = \frac{\frac{1}{K_d \cdot SSC} + 1}{\frac{Z_a}{K_d \cdot S} + 1}, \quad (2)$$

where k_{sed} and k_w are first-order biotransformation rate constants (day^{-1}) in the sediment and in the water column, respectively. Z_a and Z_w are the depths of the active sediment layer and the water column (m), respectively.

The total system biotransformation rate (k^* [day^{-1}]) is dependent on partitioning and the compartment-specific rates:

$$k^* = \frac{M_{aq} + M_{susp}}{M_{total}} k_w + \frac{M_{settl}}{M_{total}} k_{sed}. \quad (3)$$

This, relative to k_w becomes (for detailed derivation see section S2 in the SI):

$$\frac{k^*}{k_w} = \frac{\frac{A}{B} + 1}{\frac{A}{B} + 1 + \frac{E}{F}} \left(1 + \frac{\frac{E}{F}}{\frac{A}{B} \frac{F}{E} \frac{Z_a}{Z_w} + 1} \right) = \frac{\frac{1}{K_d \cdot SSC} + 1}{\frac{1}{K_d \cdot SSC} + 1 + \frac{S}{SSC \cdot Z_w}} \left(1 + \frac{\frac{S}{SSC \cdot Z_w}}{\frac{Z_a}{K_d \cdot S} + 1} \right). \quad (4)$$

Multiplying equations (1) and (4) yields the sediment modification factor (δ [–]) for a single stream reach, which expresses the relative surplus biodegradation due to the presence and activity of the settled sediment (through both retention and degradation):

$$\delta = \frac{k^* \tau^*}{k_w \tau_w} = 1 + \frac{\frac{E}{F}}{\frac{A}{B} \frac{F}{E} \frac{Z_a}{Z_w} + 1} = 1 + \frac{\frac{S}{SSC \cdot Z_w}}{\frac{Z_a}{K_d \cdot S} + 1}, \quad (5)$$

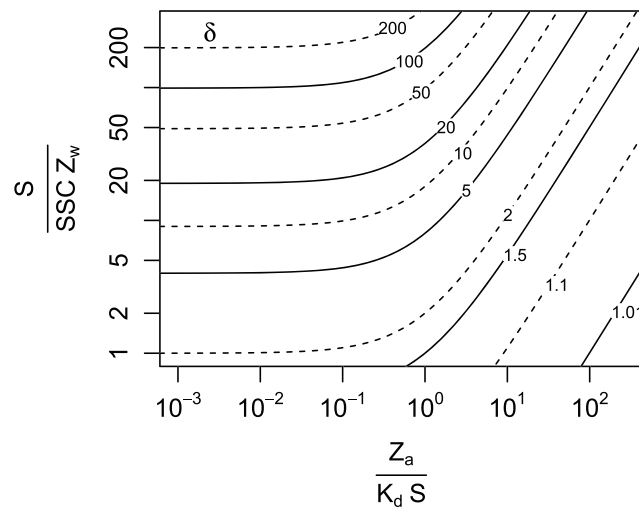


Figure 2. The role of the sediment regime and sorption properties on the sediment modification factor (δ). $\frac{S}{SSC \cdot Z_w}$ is the ratio between the settled and resuspended sediment mass; $\frac{Z_a}{K_d \cdot S}$ is the aqueous-sorbed ratio of the API in the sediment. The δ is the relative pace of biotransformation in a river reach relative to degradation in the water column alone. SSC = suspended sediment concentration.

where $\frac{S}{SSC \cdot Z_w}$ indicates the partitioning of the total sediment mass between the floating and settled phases and $\frac{Z_a}{K_d \cdot S}$ is the aqueous-sorbed ratio inside the sediment. A detailed derivation of δ in terms of A/B and E/F is presented in section S2 in the SI. If degradation pathways other than biotransformation (e.g., phototransformation or hydrolysis) are present, the equation determining δ needs some extension, but the model remains conceptually the same (see section S3 in the SI).

A value of $\delta = 2$ indicates that biotransformation of a compound in a river reach is twice what it would be in the absence of suspended and settled sediment. Stream properties and sediment dynamics can easily raise δ far beyond 1 (Figure 2) at almost any sorption behavior. Interestingly, the water-sediment depth ratio (Z_w/Z_a) does not directly influence the dimensionless travel time (equation (1)), but it plays a role in k^*/k_w and δ , especially for moderately hydrophobic compounds (Figure S3 in the supporting information). The resuspension-settling equilibrium (E/F or $\frac{S}{SSC \cdot Z_w}$) seems to be the strongest factor affecting δ . Reaches of limited resuspension capacity (i.e., with large settled-resuspended ratio) degrade strongly sorbing compounds up to orders of magnitude faster than those having restricted sediment retention ability (Figure 2).

As δ accounts for degradation outside the water column, the output flux from the reach can be calculated by putting δ inside the equation describing a reach reactor without sediment:

$$F_{out} = F_{in} \exp(-\delta k_w \tau_w), \quad (6)$$

where F_{in} and F_{out} are the total incoming and outflowing fluxes of the parent compound for a single reach (kg/day), respectively.

2.2. Model of the Stream Network

The stream network was built up from river reaches. Local API removal was calculated in each reach according to the local value of k_w , δ , and τ_w . Since the model was first-order, the downstream effect of each pollution source could be computed independently and summed.

Inputs to the stream network are uncertain. While consumption patterns for the selected APIs can be assumed to vary little by region (within a single country), excretion rates and removal rates by WWTPs are more uncertain. Therefore, to separate the uncertain proportion that never reaches the streams, the local input flux ($F_{in,local}$ [kg/day]) was written as the product of local consumption ($F_{cons,local}$ [kg/day]) and a unified escape rate ($k_{esc} = k_{excr} (1 - k_{rem})$ [-], the product of the mean human excretion rate (k_{excr}) and the proportion passing through the WWTP ($1 - k_{rem}$)):

$$F_{in,local} = F_{cons,local} k_{esc}. \quad (7)$$



Figure 3. The Rhine catchment above the Dutch-German border, major rivers, and sampling locations (open circles). The open triangle shows the upstream starting point of the profile in Figure 7.

Model inputs were the following:

1. A database of the 18,240 reaches of the Rhine catchment upstream of the Dutch border (Bimmen) from the CCM2 river and catchment database (EU JRC, <http://ccm.jrc.ec.europa.eu/>, Figure 3). Strahler stream order, drainage area (km^2), channel slope rounded to integer percent, reach length, and ID of the downstream neighbor reach were given for each reach. Due to the very coarse resolution of channel slope data, slope values were averaged across neighboring stream reaches weighted by drainage area (so that smaller steep streams cannot bias the mean slope of major rivers).
2. A table with consumption amounts for the selected APIs for each reach from the CrossWater project (Moser et al., 2018).
3. A table with the observed weekly mean flux of the selected APIs for 16 sites from the Rhine and major incoming tributaries by Ruff et al. (2015; Figure 3).

A preprocessing step was carried out once to estimate mean physical properties for each reach based on drainage area and channel slope (see description in section S4 in the SI; Andreadis et al., 2013; Mosley & McKerchar, 1993; Simons & Albertson, 1960; Wharton et al., 1989). Estimated channel geometry, flow velocity, and sediment grain size distribution had to be used due to lack of measurements in sufficient density to cover the entire stream network. Mean SSCs were derived from these parameters (see section S4 in the SI; Arcement & Schneider, 1989; Ferguson & Church, 2004; van Rijn, 1984). In reality SSC is governed by discharge, season, the state of the upstream catchment, and the stage of flood pulses, which together make it highly dynamic. We had to neglect this variability as we had no means to model dynamic SSC in the entire stream network. Products of the preprocessing step were first the water depth (Z_w), the mean flow velocity (U), the mean water residence time in the reach (τ_w), the settled sediment stock (S), SSC, the sediment mass median diameter (D_{50}), and finally E/F and Z_a/Z_w .

Calibrated model parameters were those where significant uncertainty was expected: K_d , k'_{bio} , and k_{esc} . K_d is weakly known for such a large and diverse system. It can be calculated as the product of $f_{\text{oc, sed}}$ (sediment

organic carbon content [–]) and K_{oc} (the organic carbon-water partition coefficient, [L/kg_{OC}]), but reported K_{oc} values from regulatory and other studies show high variability. The k'_{bio} was the primary target of our investigations. Values were extracted from OECD 308 studies for APIs wherever available, but they were at least as uncertain as K_d . The k_{esc} encapsulates all API-related input uncertainty, including errors in consumption rates, excretion rates, and uncertainty and variability in WWTP removal rates. The independent, normally distributed model error's standard deviation was calibrated together with the model parameters.

In each model run, the model first calculated the values of A/B and δ for every single reach. This was necessary because these quantities depend on K_d , which is calibrated. After this, traveling fluxes of APIs were calculated for each reach by assuming both degradation and conservative behavior. The likelihood of model parameters was calculated at reaches where measurements were available.

The calibration procedure took place in a Bayesian framework. An informative prior was assigned to k_{esc} : a lognormal distribution with the estimated mean values from Singer et al. (2016) with a relative standard deviation of 15%, except for API13, where the published value for k_{esc} was too low to justify the observations along the Rhine and therefore a uniform distribution over the [0,1] domain was used ($k_{esc} = 0.25$ was necessary instead of 0.09 to produce the observed flux without any degradation). The prior for K_{oc} was a lognormal distribution with mean from OECD 106 experiments and 80% relative standard deviation. The prior for k'_{bio} was a uniform distribution over the technically feasible numerical range (10^{-4} to 10^4 [L (days·g·OC)⁻¹]) to prevent mathematical instability. The parameter posterior was sampled by Markov chain Monte Carlo sampling.

2.3. Model of OECD 308 Experiments

The model of Honti et al. (2016) was applied to obtain k'_{bio} from 10 OECD 308 experiments featuring the four compounds API6, API8, API9, and API13. Data were extracted from confidential dossiers provided by the German Environment Agency (Fenner et al., 2016). Concentration-time series were derived from duplicate measurements by averaging. Experimental metadata belonging to or required for interpretation of OECD 308 were extracted from the dossiers as well, such as results of OECD 106 sorption experiments. Calibration again took place in a Bayesian framework; the same priors were used for K_{oc} and k'_{bio} as in the calibration of the stream network model.

3. Results

3.1. Degradation of APIs in the Rhine Basin

Simulated longitudinal profiles of API fluxes were in good agreement with the measurements for all APIs (Figures 4, S7, and S8 in the SI). Given that Ruff et al. (2015) report about 20% measurement accuracy, calibration fulfilled expectations. The only significant discrepancy between measured and modeled values was the model's inability to fit to a probably erroneous measured point for API8. Less severe, yet systematic deviations were observed at the last measurement point (Bimmen). Here the model was overestimating the local flux for all compounds except API8 by 5% to 25%. Possible explanations for this systematic error are (i) errors in the physical calculations for the lowermost sections of the Rhine affecting flow velocities or SSCs, (ii) regional deviations in the load/emission data, or (iii) incomplete mixing of shoreline plumes or cross sectionally not representative sampling.

Out of the seven APIs, two showed fast and efficient degradation in the stream network (API6 and TTP), one was moderately degrading (API9), and three were practically conservative (CMZ, API8, and SIG; Figure 5). Due to the uncertainty of k_{esc} , the modeled degradation of API13 varied between limited and moderate. Based on previous experience, CMZ was expected to be conservative, which was not contradicted by the model results (but API8 and SIG were even *more conservative*, showing even less degradation).

There was a clear relationship between simulated degradation in the stream network and the calibrated Rhine k'_{bio} values, which was no surprise considering the model mechanisms. Differences in sorption properties of the individual compounds did not strongly influence the correspondence between k'_{bio} and degradation. Below the k'_{bio} value of 40 [L (days·g·OC)⁻¹] compounds were not degraded noticeably. Values above 200 led to 80–90% degradation.

One noteworthy aspect is that measured longitudinal flux profiles of both conservative and degrading compounds look very similar; that is, there is a pattern of increasing load downstream (Figures 4 and 7). This behavior was well mirrored by the modeled profiles. The reason that degradation did not leave a recognizable imprint on the shape of the profile in the Rhine river is that—according to the model—none of the com-

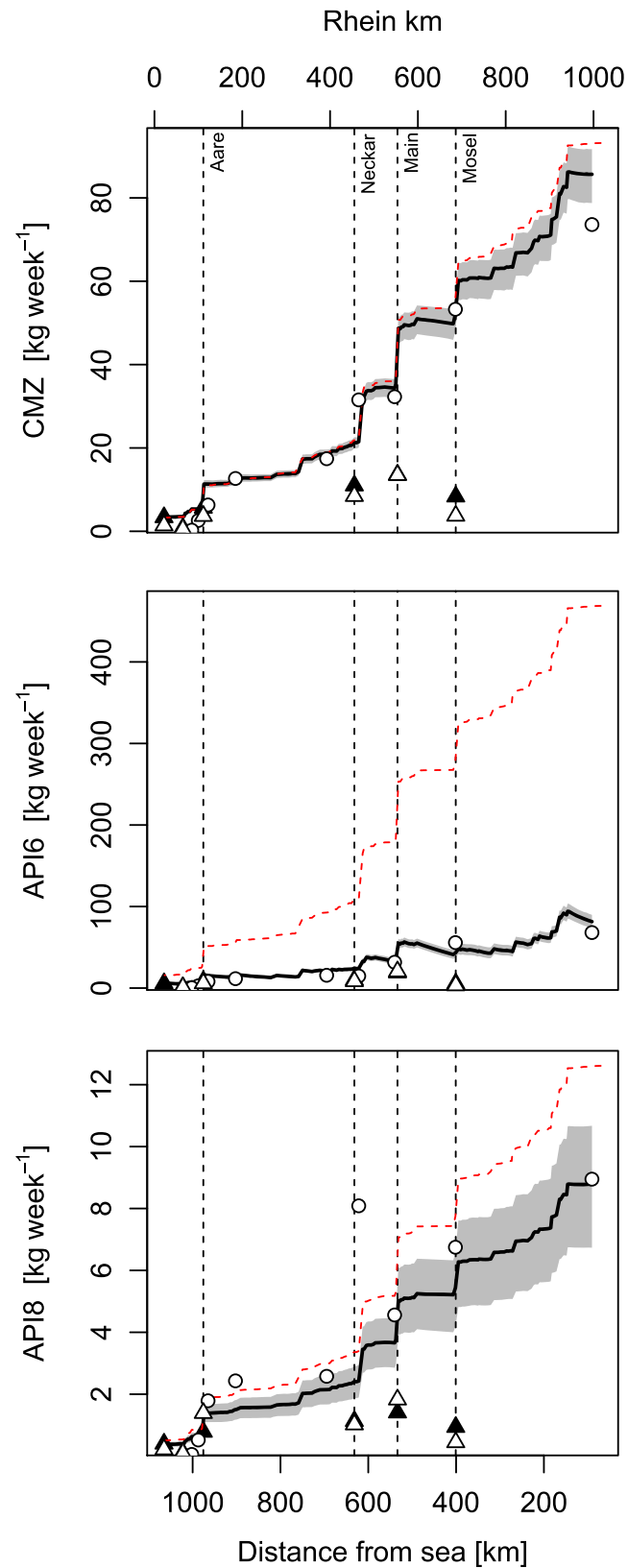


Figure 4. Modeled and measured flux profiles of selected APIs along the Rhine. Open symbols: measurements (circles: Rhine, triangles: tributaries), closed triangles: modeled values for tributary inflows. Climbing dashed line: conservative assumption (accumulated load). Black line: best model fit. Gray band: 95% uncertainty interval. Note: open triangles may hide closed ones on perfect coincidence. API = active pharmaceutical ingredient;

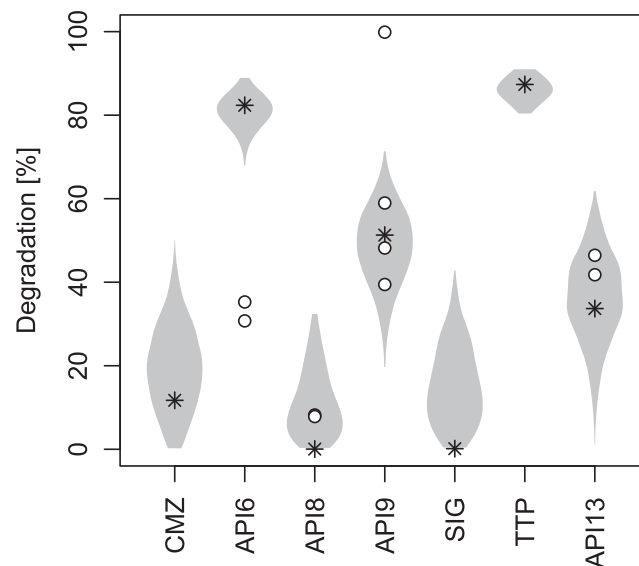


Figure 5. Modeled total degradation of APIs in the Rhine basin (violins, with asterisk indicating the maximum likelihood values) and in OECD 308 experiments (open dots, values at 14 days after experiment start). CMZ = carbamazepine; API = active pharmaceutical ingredient; SIG = sitagliptin; TTP = trimethoprim; OECD = Organisation for Economic Co-operation and Development.

pounds degraded significantly in higher-order streams (over Strahler orders 5–6), especially not in the Rhine itself (Figure 7). The model suggests that if there was any degradation, it rather happened in the small- and medium-sized streams (up to Strahler order 4). In the higher-order streams the high Z_w/Z_a ratio and low SSC (see Figure S5 in the supporting information) prevented significant biotransformation. In addition to this physical dependence on stream size, the majority of emission sources concentrate around lower-order reaches (Figure 8, top). Due to the lack of degradation in the Rhine, the incoming tributary loads are largely preserved until the outflow, regardless of the compound's degradability, and hence accumulate along the Rhine. As a

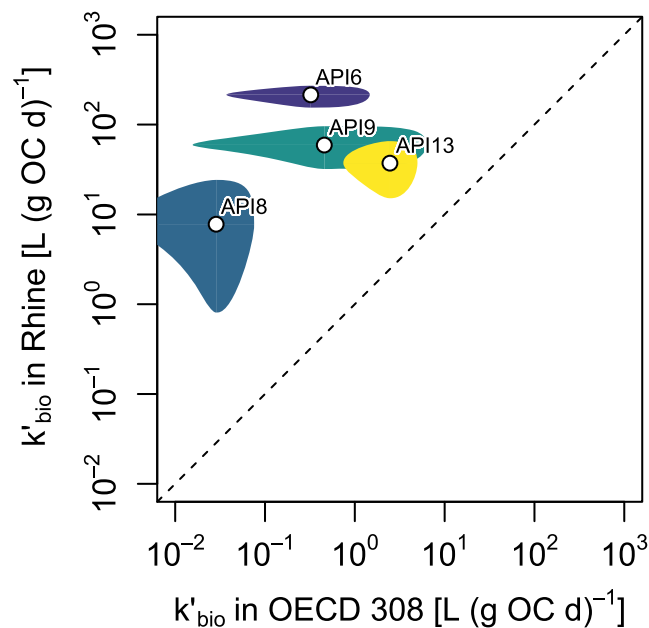


Figure 6. Relationship between k'_{bio} in the Rhine basin and k'_{bio} derived from OECD 308 and field data. The dashed line indicates the 1:1 line. API = active pharmaceutical ingredient; OECD = Organisation for Economic Co-operation and Development.

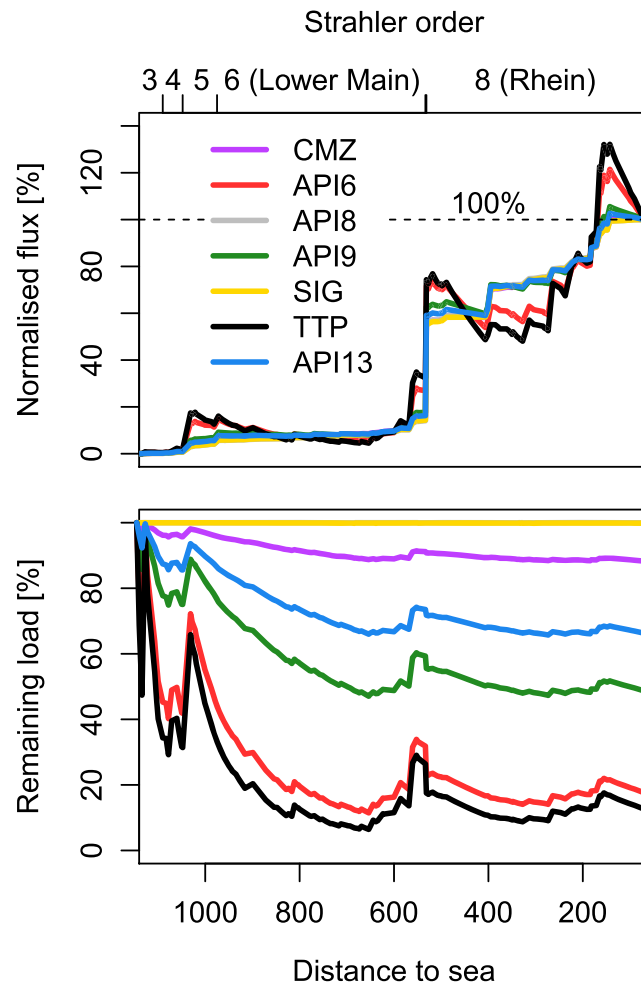


Figure 7. Modeled downstream profile through River Rednitz, River Main, and the Rhine starting from near Ansbach. (top) Flux of APIs normalized by the value at Bimmen. (bottom) Proportion of the total upstream load remaining in the river. The jump from Strahler order 6 to 8 is the confluence with the Rhine at Mainz; the jump from 4 to 5 is the confluence with the Main at Bamberg. CMZ = carbamazepine; API = active pharmaceutical ingredient; SIG = sitagliptin; TTP = trimethoprim.

result, loads of wastewater-related contaminants in the Rhine roughly scale with catchment area and hence steadily grow along the river.

Based on the calculated A/B , E/F , and Z_a/Z_w values of the stream reaches, δ was typically in the range of 4–13 (90% range). This indicates that the total system degradation was everywhere much faster than degradation in water alone. This is in line with the experience gained in laboratory water-sediment systems, such as OECD 308 and 309 (Honti & Fenner, 2015; Honti et al., 2016; Shrestha et al., 2016). However, due to the usually very low rate of degradation in water, such high multiplier values still could not guarantee that the overall degradation was observable in all parts of the stream network. The pace of degradation relative to k'_{bio} ($\frac{k^*}{k'_{\text{bio}}} \approx \delta \text{ SSC}$) followed a rather simple pattern everywhere. It was proportional to the inverse of water depth (Z_w^{-1} , Figure 8). Such a close relationship between Z_w^{-1} and $\delta \text{ SSC}$ is probably case specific and was caused by the lack of physical data from the stream network. As all reach parameters were inferred from the two numbers for drainage area and slope, we must have underestimated the physical variability among similarly sized reaches and consequently the variability in their degradation capacity.

3.2. Comparison to Degradation in OECD 308 Systems

The k'_{bio} values from OECD 308 experiments were lower than the values deduced from field data for all four compounds having both types of data (Figure 6). The difference can presumably be attributed to the fact that APIs were exposed to more diverse degraders and degradation pathways during their travel in the Rhine basin

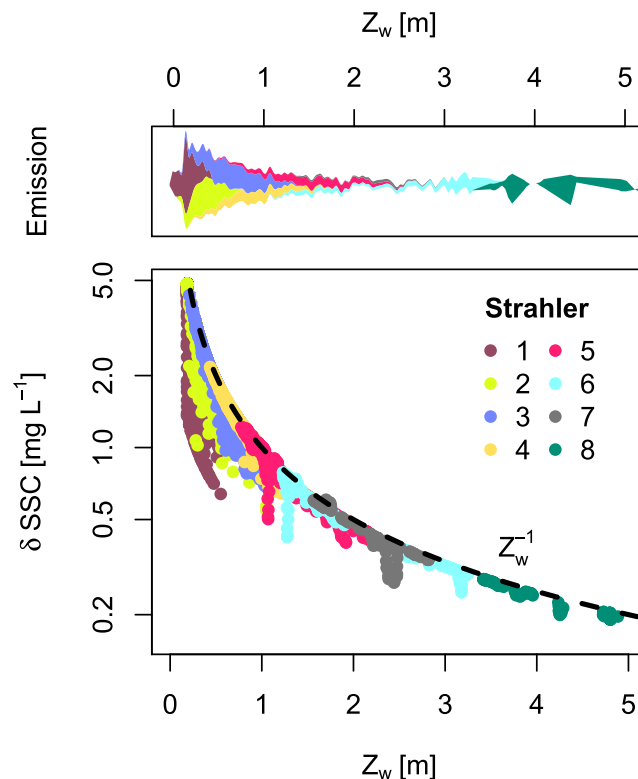


Figure 8. The role of water depth (Z_w) in the modeled relative degradation rate constants (δ SSC). Colors indicate the Strahler stream order of reaches; the upper panel shows a streamplot of emissions into the differently sized and ordered reaches (the local height of patches is proportional to the emission in grams per day).

than during being trapped in the closed experimental vessels (i.e., deeper oxic layers due to turbulence, more exchange between settled and suspended phase, and more diverse microbial communities). To more directly evaluate the outcome of OECD 308 experiments against field observations, we also sought to directly compare degradation between the two systems. We found that degradation in the Rhine catchment (upstream of Bimmen) and during approximately the first 14 days of the OECD 308 experiments generally showed qualitative agreement (Figure 5). The 14-day period was selected because it was comparable to the mean residence time in the Rhine basin (free flowing time: 7 days) and being reported in the OECD 308 dossiers of all four compounds. The only exception from the qualitative agreement was API6 that showed only about half the degradation in the OECD 308 experiment compared to its degradation in the Rhine, suggesting additional degradation mechanisms that are not present in simulation tests but are relevant in the field, for example, direct or indirect photolysis. This is also reflected by the fact that API6 shows the highest discrepancy between field and experimental k'_{bio} among the four compounds for which this comparison was possible. It needs to be kept in mind though that the above comparisons are not very robust due to the problems of identifying k'_{bio} from field data (see below) and the high variability of k'_{bio} values derived from OECD 308 data. The latter is nicely illustrated by API9: Degradation in OECD 308 by day 14 varied between 59% and 99% for two experiments carried out with the very same sediment.

3.3. Importance of Input Uncertainty

The increasing longitudinal flux profiles cause a practical problem. As the smaller streams where the majority of degradation takes place are much shorter than the large rivers, the corresponding flux profiles taken from the Rhine (or main rivers) all resemble the profile of a conservative compound. Therefore, when the actual emission rates of a certain API from WWTPs are not or only weakly known, uncertainty heavily influences the inferred degradation rates, causing a strong positive correlation between k_{esc} and k'_{bio} (Figure S6 in the supporting information). This is possible because the degrading and nondegrading profiles show only small differences (Figure 7, top) that can easily remain unnoticed when measurement points are sparsely distributed and flux estimations have an admitted accuracy of about 20%.

4. Discussion

4.1. Biodegradation in the Rhine and in the Laboratory

The systematically larger k'_{bio} values from the Rhine basin compared to OECD 308 experiments could be logically interpreted as the result of reduced microbial diversity and the ensuing lack of certain transformation pathways in the experimental systems.

The comparison of field-laboratory rates for abiotic processes often come up with the opposite conclusion: Well-mixed laboratory systems show higher complexing, weathering, and dissolution rate constants than soil profiles or natural sediment columns (Liu et al., 2013; Wen & Li, 2018; Pačes, 1983; Swoboda-Colberg & Drever, 1993) due to hindrances of mass transfer and higher spatial heterogeneity in the field. The case of biotransformation and OECD 308 is somewhat different. From the physical side, contrary to the abiotic systems cited above, the stagnant OECD 308 is obviously less well mixed than any stream, so the mass transfer would be more effective in the field, facilitating a faster degradation. From the chemical side, the sediment of OECD 308 is anaerobic except for a very thin surface layer, which decreases the number of potential transformation pathways for most APIs, while stream sediments are typically aerobic in the first few centimeters. OECD 308 must be performed in darkness, which excludes the possibility of phototransformation, while streams are at least partially exposed to sunlight. From the biological side, microbial diversity is a key factor in biotransformation of organic micropollutants, and therefore, higher physical and chemical heterogeneity—which are evidences for ineffective mass transfer yet support higher microbial diversity—should basically increase the number of transformation pathways. The preincubation of the OECD 308 system before spiking the API is likely to exert a strong selective pressure on the microbiota, lowering diversity, and thereby the number of effective heterotrophic transformation pathways. These factors altogether mean that OECD 308 suffers from both mass transfer limitation and a relative scarcity of transformation pathways, which explains observing lower first-order degradation rate constants and longer half-lives.

However, it has to be noted that both sets of calibrated biotransformation rate constants are conditional on the structures of the corresponding mathematical models. Potential structural deficiencies—like a missing mechanism, for example, phototransformation—and wrong parameterizations—like biased expectations on certain parameters—can also produce systematic deviations between the two sets. As no model is surely free from such defects, it cannot be proven whether the apparently higher degradation rate constants of the Rhine indeed reflect the effect of the better mixed yet still more diverse stream environment.

Nevertheless, we have found qualitative agreement between degradation in the first 14 days of OECD 308 and degradation in the Rhine basin upstream of Bimmen (Figure 5), but the small number of involved compounds did not allow us to judge the strength of this agreement statistically. While extending the analysis to more compounds could fix the statistical issue and prove or refute this specific agreement, other subcatchments in the Rhine basin or other river basins would certainly show different relationships. Other catchments with different catchment size, distribution of stream orders, reach length, residence time, and sediment conditions would potentially remove different amounts of APIs. However, the model suggests that there is a reduction in differences between sufficiently large river basins in terms of API removal. As biotransformation concentrates in small- and medium-sized streams, one can expect that total removal does not increase linearly with stream length and basin size. Our model showed that after 1–2 days of mean water residence time (approximately 2–4 days free flowing time from the most distant source to the subcatchment outlet) subcatchment-specific removal rates stabilize. This coincides with the onset of stream orders 6–7. Therefore, if other conditions were similar, basins with a main river over Strahler order 6 should have more similar removal rates than smaller ones. Therefore, if a simulation test represents degradation in a large river basin, from a physical point of view it is likely to represent other large basins as well.

4.2. Representativeness of Simulation Tests

In the limited spectrum of physical properties represented by the modeled reaches of the Rhine, stream network degradation could vary between extremely slow (in the major channels) and rather fast (headwaters) for the same compound. Such high variability of the actual in-stream degradation highlights that it is illusory to think that experimentally derived half-lives represent at least a considerable proportion of the environment. According to our model, half-lives can vary over orders of magnitude in the stream network due to the different physical properties of stream reaches (Figures 2 and S3), while we did not even consider changes in microbial community composition along the stream network. Simulation tests such as OECD 308 and 309

define very specific conditions and therefore are able to simulate the compound's behavior in tiny niches of the environmental spectrum.

Thus, instead of the current risk assessment practice of projecting experimental half-lives to the environment in general, it would be preferable to view simulation tests as more (OECD 308) or less (varieties of OECD 309) standardized ways of deducing environment-invariant properties of the compound (such as k'_{bio} , or A/B) that can afterward be used to estimate half-lives under different environmental conditions.

In this respect, however, both OECD 308 and 309 suffer from serious drawbacks. Beyond their considerable costs and effort requirements, they fail to provide relevant information for persistence modeling in most kinds of streams. The presented model can be used to demonstrate this, but findings are not conditional on the model assumptions. In the current model, A/B and E/F are the most important physical (partitioning) factors modulating the rate of degradation. Even when carried out with the sediment in question, OECD 308 does not provide useful information on any of them: There is hardly any suspended sediment in the water column of OECD 308 experiments, so sorption to suspended solids (from which A/B could be derived) or partitioning between suspended and settled phases (E/F) cannot be measured. Instead, sorption influences the compound's distribution inside the sediment and, as a consequence, diffusion between the water and sediment layers, yet these processes are difficult to extract from the measured concentration patterns. Accordingly, while k'_{bio} can be derived from OECD 308, it is quite uncertain due to the interaction between these processes (Honti et al., 2016). While it is not surprising that the stagnant OECD 308 experiments does not represent streams too well, the problems of OECD 309 experiments in doing so are more surprising. In the nonpelagic versions of OECD 309, there is sorption to suspended sediment, and hence, A/B and its effect on k'_{bio} should theoretically be observable. However, since SSCs in such systems are quite low, biodegradation is rather limited in practice. As a consequence, while information can be gained on A/B , there is little information to be learned on k'_{bio} from these experiments. Thus, OECD 309 experiments tend to be very expensive hydrolysis experiments rather than actual biodegradation tests. Moreover, because the sediment is kept in suspension in these experiments, there is no way to learn anything about the influence of settling (i.e., E/F) on degradation.

From a modeling perspective, a hybrid (flume or stirred) experiment with both suspended particles and settled sediment could be a better solution. By carrying out such experiments with different settings (different SSC—but enough to stimulate observable degradation, S), one could determine all critical model parameters with reasonable accuracy.

4.3. Behavior of Stream Networks and Input Uncertainty

According to our model, whenever degradation happened, it was in the small and medium tributaries. Large streams acted as conveyor belts forwarding all incoming pollution toward the North Sea. Boeije (2000) found the same with GREAT-ER on a different basis: They attributed degradation in the sediment entirely to surface biofilms (which may not be a proper assumption in larger, deep streams) and concluded that increasing stream size reduces exposure to sediment and therefore elongates half-lives. Half-lives in small creeks can be 60 times shorter than in large rivers (Boeije, 2000). The cross-sectional area-volume ratios identified as primary physical determinants of degradation half-lives by Boeije (2000) are equivalent to the hydraulic radius, which is approximately equal to Z_w in natural channels (cf. Figure 8). The negative scaling of biodegradation potential with stream size is not limited to micropollutants. Alexander et al. (2000) found similar patterns for nitrogen.

Considering the suggested place of degradation (small to medium streams), the positions of measurement locations were suboptimal. As all points were along the Rhine, in either the Rhine itself or in the mouths of major tributaries, measured fluxes bore no information about what happened in the upstream focal regions of degradation. One could argue that measurement locations should have been positioned in smaller streams as well, but there is the aspect of size, too. The upstream catchment above a measurement location must be large enough to smooth out temporal and spatial variability of pollution sources and must host enough inhabitants to produce a clear chemical signal. Therefore, the placement of measurement locations needs a careful balancing. Starting and endpoints of longer sections of medium-sized tributaries without significant lateral inputs could be optimal points for future sampling campaigns.

As we found no way to infer degradation from the observed fluxes alone, the model's findings about degradation are conditional on the input data: the national consumption statistics and the estimated consumer excretion and WWTP removal rates taken from Singer et al. (2016).

For conservative APIs we found that the emissions calculated from consumption data from Moser et al. (2018) and the consumer excretion rates plus WWTP removal rates from Singer et al. (2016) nicely matched the observed flux data of Ruff et al. (2015) for almost each measurement point. This fact makes the same likely for the degrading compounds, thereby indirectly supporting our statements on the extent and place of degradation.

The difficulty of separating emissions from degradation has already been described by Pistocchi et al. (2012) in the context of a totally different model framework. They also concluded that emission-half-life combinations can be identified but none of them separately. Knowledge of either is necessary to estimate the other from field data.

For large river systems, pollutants will make the majority of their travel (distance wise) inevitably in large streams. Due to the accumulating nature of large rivers, this means that sampling along the main channels will reflect a picture that is very similar to the behavior of a conservative compound. This suggests that, for compounds without a solid consumption and emission data foundation, the estimation of degradation parameters can become impossible.

4.4. Sediment Behavior

Sediment dynamics is a cornerstone of our model, as it influences δ via E/F . According to the SSC estimation method described in section S4, the streams of the Rhine basin seem to be generally sediment poor. Suspended loads are far below the hydraulic carrying capacity of flow (see section S4 in the SI; ; Maniak, 2010; Schmidt & Unbenannt, 2003; TK Consult AG, 2013). Internal sediment supply is the only possible major supplier of SSC during low and medium flow when surface runoff is negligible. Compared to common definitions of the *active* sediment layer from a sedimentology perspective (about 3 times the 90th percentile grain size diameter $[D_{90}]$ or the median grainsize diameter $[D_{50}]$), even such low SSCs require intensive exchange between the water column and the active layer. In that case, however, the common concept of the sediment as a relatively stable sink for pollutants is wrong. A simple calculation can estimate the order of magnitude of residence times in the active layer. An average sand particle with $D = 0.5$ mm has a terminal settling velocity around 5–10 cm/s. Considering an SSC of 30 (mg/L), and $Z = 5$ (m; all values are typical for the Rhine) the downward settling flux is about 0.002 ($\text{kg} \cdot \text{m}^{-2} \cdot \text{s}^{-1}$), which—in equilibrium—must be paired by a similar upward flux. Even with an active layer depth of $Z_a = 3$ (cm; upper limit of calculated values for stream reaches of Strahler orders 6–8), and porosity of 50%, the average particle residence time in the active layer is as little as 5 hr in steady low and medium flow. Unsteady flow and especially bed-moving floods are expected to further shorten this period. Thus, unless a protective biofilm develops altering particle exchange between the water column and the sediment (Vignaga et al., 2013), in larger streams the active layer is likely to be restructured at subdaily frequency, which is in strong contrast with a typical lake sediment and the experimental conditions in OECD 308.

5. Conclusions

- The persistence of APIs could not be evaluated from concentration patterns in the field alone. Rather, precise emission rates (consumption, consumer excretion, and removal in WWTPs) need to be known together with an approximate K_d . Otherwise emissions, sorption, and degradation can compensate for each other's effect, which renders the identification of actual degradation impossible.
- Persistence suggested by simulation tests did not robustly match persistence inferred from field observations. According to the model calibration, k'_{bio} is higher in rivers than in OECD 308, probably due to the higher variety of processes that facilitate biotransformation. Candidates for such processes are turbulence and mixing, temperature, light exposure, and higher diversity of degrader microfauna.
- Despite the higher calibrated values of k'_{bio} , the Rhine stream network cannot degrade higher proportions of emitted APIs than the first 14 days of an OECD 308 experiment. This is explained by the (i) lack of time and (ii) limited exposure to degrader biomass in the main rivers.
- Our model suggests that physical conditions seriously limit exposure to degrader biomass above Strahler stream orders 5–6. Therefore, streams of order 1–5 can be considered as hot spots for biodegradation in the Rhine basin.

Acknowledgments

The Pldent project was supported, and the OECD 308 data were provided by the German Environment Agency (Umweltbundesamt) under contract FKZ 3715 65 415 3. Emission data from the CrossWater project financed by the Swiss National Science Foundation (Grant 406140-125866) is gratefully acknowledged. Support of grant BME FIKP-VIZ by EMMI is kindly acknowledged. We thank Daniela Gildemeister and Janina Wöltjen from the German Environment Agency for their constructive comments on the manuscript. Data used in this study are available in public repositories, except for the raw OECD 308 data, which are managed by the European Medicines Agency (EMA, <https://www.ema.europa.eu/en/medicines>). Parts of the confidential applications for marketing authorization for the respective APIs are not published in the European Public Assessment Reports (EPAR) on the EMA website. GIS data on subcatchments, river segments and topology, and people equivalents are available at <https://doi.org/10.5281/zenodo.556143>, API consumption and removal in wastewater treatment plants at <https://doi.org/10.1021/acs.est.5b03332>, and monitored data in the Rhine at <https://doi.org/10.1016/j.watres.2015.09.017>.

References

- Alexander, R. B., Smith, R. A., & Schwarz, G. E. (2000). Effect of stream channel size on the delivery of nitrogen to the Gulf of Mexico. *Nature*, 403(6771), 758–761. <https://doi.org/10.1038/35001562>
- Andreadis, K. M., Schumann, G. J.-P., & Pavelsky, T. (2013). A simple global river bankfull width and depth database. *Water Resources Research*, 49, 7164–7168. <https://doi.org/10.1002/wrcr.20440>
- Arcement, G. J., & Schneider, V. R. (1989). Guide for selecting Manning's roughness coefficients for natural channels and flood plains (Tech. Rep.) Reston, VA: U. S. Geological Survey.
- Boeije, G. (2000). Incorporation of biofilm activity in river biodegradation modeling: A case study for linear alkylbenzene sulphonate (LAS). *Water Research*, 34(5), 1479–1486. [https://doi.org/10.1016/S0043-1354\(99\)00279-1](https://doi.org/10.1016/S0043-1354(99)00279-1)
- Boethling, R., Fenner, K., Howard, P., Klečka, G., Madsen, T., Snape, J. R., & Whelan, M. J. (2009). Environmental persistence of organic pollutants: Guidance for development and review of POP risk profiles. *Integrated Environmental Assessment and Management*, 5(4), 539–556. https://doi.org/10.1897/ieam_2008-090.1
- Davis, J., Gonsior, S., Marty, G., & Ariano, J. (2005). The transformation of hexabromocyclododecane in aerobic and anaerobic soils and aquatic sediments. *Water Research*, 39(6), 1075–1084. <https://doi.org/10.1016/j.watres.2004.11.024>
- Ensign, S. H., & Doyle, M. W. (2006). Nutrient spiraling in streams and river networks. *Journal of Geophysical Research*, 111, G04009. <https://doi.org/10.1029/2005JG000114>
- Ericson, J. F. (2007). An evaluation of the OECD 308 water/sediment systems for investigating the biodegradation of pharmaceuticals. *Environmental Science & Technology*, 41(16), 5803–5811. <https://doi.org/10.1021/es063043+>, PMID: 17874790.
- Ericson, J. F., Smith, R. M., Roberts, G., Hannah, B., Hoeger, B., & Ryan, J. (2013). Experiences with the OECD 308 transformation test: A human pharmaceutical perspective. *Integrated Environmental Assessment and Management*, 10(1), 114–124. <https://doi.org/10.1002/ieam.1457>
- Feijtel, T., Boeije, G., Matthies, M., Young, A., Morris, G., Gandolfi, C., et al. (1997). Development of a geography-referenced regional exposure assessment tool for European rivers—GREAT-ER contribution to GREAT-ER #1. *Chemosphere*, 34(11), 2351–2373. [https://doi.org/10.1016/S0045-6535\(97\)00048-9](https://doi.org/10.1016/S0045-6535(97)00048-9)
- Fenner, K., Honti, M., Stamm, C., Varga, L., & Bischoff, F. (2016). Suitability of laboratory simulation tests for the identification of persistence in surface waters (Tech. Rep. FKZ 3715 65 415 3). Dessau, Germany: German Environment Agency (Umweltbundesamt).
- Ferguson, R., & Church, M. (2004). A simple universal equation for grain settling velocity. *Journal of Sedimentary Research*, 74(6), 933–937. <https://doi.org/10.1306/051204740933>
- Fono, L. J., Kolodziej, E. P., & Sedlak, D. L. (2006). Attenuation of wastewater-derived contaminants in an effluent-dominated river. *Environmental Science & Technology*, 40(23), 7257–7262. <https://doi.org/10.1021/es061308e>
- Honti, M., & Fenner, K. (2015). Deriving persistence indicators from regulatory water-sediment studies – opportunities and limitations in OECD 308 data. *Environmental Science & Technology*, 49(10), 5879–5886. <https://doi.org/10.1021/acs.est.5b00788>
- Honti, M., Hahn, S., Hennecke, D., Junker, T., Shrestha, P., & Fenner, K. (2016). Bridging across OECD 308 and 309 data in search of a robust biotransformation indicator. *Environmental Science & Technology*, 50(13), 6865–6872. <https://doi.org/10.1021/acs.est.6b01097>
- Huntscha, S., Singer, H., Canonica, S., Schwarzenbach, R. P., & Fenner, K. (2008). Input dynamics and fate in surface water of the herbicide metolachlor and of its highly mobile transformation product metolachlor ESA. *Environmental Science & Technology*, 42(15), 5507–5513. <https://doi.org/10.1021/es800395c>
- Ingold, K., Moser, A., Metz, F., Herzog, L., Bader, H.-P., Scheidegger, R., & Stamm, C. (2018). Misfit between physical affectedness and regulatory embeddedness: The case of drinking water supply along the Rhine River. *Global Environmental Change*, 48, 136–150. <https://doi.org/10.1016/j.gloenvcha.2017.11.006>
- Koormann, F., Rominger, J., Schowanek, D., Wagner, J.-O., Schröder, R., Wind, T., et al. (2006). Modeling the fate of down-the-drain chemicals in rivers: An improved software for GREAT-ER. *Environmental Modelling & Software*, 21(7), 925–936. <https://doi.org/10.1016/j.envsoft.2005.04.009>
- Kunkel, U., & Radke, M. (2008). Biodegradation of acidic pharmaceuticals in bed sediments: Insight from a laboratory experiment. *Environmental Science & Technology*, 42(19), 7273–7279. <https://doi.org/10.1021/es801562j>
- Li, Z., Sobek, A., & Radke, M. (2015). Flume experiments to investigate the environmental fate of pharmaceuticals and their transformation products in streams. *Environmental Science & Technology*, 49(10), 6009–6017. <https://doi.org/10.1021/acs.est.5b00273>
- Liber, K., Solomon, K. R., & Carey, J. H. (1997). Persistence and fate of 2,3,4,6-tetrachlorophenol and pentachlorophenol in limnocoarals. *Environmental Toxicology and Chemistry*, 16(2), 293–305. <https://doi.org/10.1002/etc.5620160227>
- Lindim, C., van Gils, J., & Cousins, I. (2016). A large-scale model for simulating the fate & transport of organic contaminants in river basins. *Chemosphere*, 144, 803–810. <https://doi.org/10.1016/j.chemosphere.2015.09.051>
- Liu, C., Shang, J., Kerisit, S., Zachara, J. M., & Zhu, W. (2013). Scale-dependent rates of uranyl surface complexation reaction in sediments. *Geochimica et Cosmochimica Acta*, 105, 326–341. <https://doi.org/10.1016/j.gca.2012.12.003>
- Maniak, U. (2010). *Hydrologie und Wasserwirtschaft: Eine Einführung für Ingenieure*. Heidelberg: Springer Berlin. <https://doi.org/10.1007/978-3-642-05396-2>
- Moser, A., Wemyss, D., Scheidegger, R., Fenicia, F., Honti, M., & Stamm, C. (2018). Modelling biocide and herbicide concentrations in catchments of the Rhine basin. *Hydrology and Earth System Sciences*, 22(8), 4229–4249. <https://doi.org/10.5194/hess-22-4229-2018>
- Mosley, M. P., & McKerchar, A. I. (1993). Chapter 8: Streamflow. In D. R. Maidment (Ed.), *Handbook of hydrology* (Chap. 8, pp. 8.1–8.39). New York: McGraw-Hill Education.
- Newbold, J. D., Elwood, J. W., O'Neill, R. V., & Winkle, W. V. (1981). Measuring nutrient spiraling in streams. *Canadian Journal of Fisheries and Aquatic Sciences*, 38(7), 860–863. <https://doi.org/10.1139/f81-114>
- Pačes, T. (1983). Rate constants of dissolution derived from the measurements of mass balance in hydrological catchments. *Geochimica et Cosmochimica Acta*, 47(11), 1855–1863. [https://doi.org/10.1016/0016-7037\(83\)90202-8](https://doi.org/10.1016/0016-7037(83)90202-8)
- Pistocchi, A., Marinov, D., Pontes, S., & Gawlik, B. M. (2012). Continental scale inverse modeling of common organic water contaminants in European rivers. *Environmental Pollution*, 162, 159–167. <https://doi.org/10.1016/j.envpol.2011.10.031>
- Radke, M., & Maier, M. P. (2014). Lessons learned from water/sediment-testing of pharmaceuticals. *Water Research*, 55, 63–73. <https://doi.org/10.1016/j.watres.2014.02.012>
- Ruff, M., Mueller, M. S., Loos, M., & Singer, H. P. (2015). Quantitative target and systematic non-target analysis of polar organic micro-pollutants along the river Rhine using high-resolution mass-spectrometry—Identification of unknown sources and compounds. *Water Research*, 87, 145–154. <https://doi.org/10.1016/j.watres.2015.09.017>
- Schmidt, K.-H., & Unbenannt, M. (2003). Schwebstofftransport—die Fließgewässer als Transportbänder. In S. Tzschaschel (Ed.), *Nationalatlas Bundesrepublik Deutschland—Band 2, Natur und Umwelt I: Relief, Boden und Wasser* (pp. 136–137). Leipzig, Germany: Institut für Länderkunde".

- Schwarzenbach, R. P., Gschwend, P. M., & Imboden, D. M. (2016). *Environmental organic chemistry*, 3rd edition. NJ: John Wiley.
- Shrestha, P., Junker, T., Fenner, K., Hahn, S., Honti, M., Bakkour, R., et al. (2016). Simulation studies to explore biodegradation in water-sediment systems: From OECD 308 to OECD 309. *Environmental Science & Technology*, 50(13), 6856–6864. <https://doi.org/10.1021/acs.est.6b01095>
- Simons, D. B., & Albertson, M. L. (1960). Uniform water conveyance channels in alluvial materials. *ASCE Journal of the Hydraulics Division*, 86(5), 33–71.
- Singer, H. P., Wössner, A. E., McArdell, C. S., & Fenner, K. (2016). Rapid screening for exposure to “non-target” pharmaceuticals from wastewater effluents by combining HRMS-based suspect screening and exposure modeling. *Environmental Science & Technology*, 50(13), 6698–6707. <https://doi.org/10.1021/acs.est.5b03332>
- Solomon, K. R., Yoo, J. Y., Lean, D., Kaushik, N. K., Day, K. E., & Stephenson, G. L. (1985). Dissipation of permethrin in limnocoarals. *Canadian Journal of Fisheries and Aquatic Sciences*, 42(1), 70–76. <https://doi.org/10.1139/f85-009>
- Swoboda-Colberg, N. G., & Drever, J. I. (1993). Mineral dissolution rates in plot-scale field and laboratory experiments. *Chemical Geology*, 105(1–3), 51–69. [https://doi.org/10.1016/0009-2541\(93\)90118-3](https://doi.org/10.1016/0009-2541(93)90118-3)
- TK Consult AG (2013). Überflutung Beznau – Ermittlung der maximalen Überflutungshöhe der Beznau-Insel unter Berücksichtigung von Feststofftransport (Tech. Rep.) Zürich, Switzerland: Eidgenössisches Nuklearsicherheitsinspektorat ENSI.
- Tixier, C., Singer, H. P., Canonica, S., & Müller, S. R. (2002). Phototransformation of triclosan in surface waters: A relevant elimination process for this widely used BiocideLaboratory studies, field measurements, and modeling. *Environmental Science & Technology*, 36(16), 3482–3489. <https://doi.org/10.1021/es025647t>
- Tixier, C., Singer, H. P., Oellers, S., & Müller, S. R. (2003). Occurrence and fate of carbamazepine, clofibric acid, diclofenac, ibuprofen, ketoprofen, and naproxen in surface waters. *Environmental Science & Technology*, 37(6), 1061–1068. <https://doi.org/10.1021/es025834r>
- Trapp, S., & Matthies, M. (1998). *Chemodynamics and environmental modeling*. Heidelberg: Springer Berlin. <https://doi.org/10.1007/978-3-642-80429-8>
- van Rijn, L. C. (1984). Sediment transport, Part II: Suspended load transport. *Journal of Hydraulic Engineering*, 110(11), 1613–1641. [https://doi.org/10.1061/\(asce\)0733-9429\(1984\)110:11\(1613\)](https://doi.org/10.1061/(asce)0733-9429(1984)110:11(1613))
- Vignaga, E., Sloan, D. M., Luo, X., Haynes, H., Phoenix, V. R., & Sloan, W. T. (2013). Erosion of biofilm-bound fluvial sediments. *Nature Geoscience*, 6(9), 770–774. <https://doi.org/10.1038/ngeo1891>
- Wen, H., & Li, L. (2018). An upscaled rate law for mineral dissolution in heterogeneous media: The role of time and length scales. *Geochimica et Cosmochimica Acta*, 235, 1–20. <https://doi.org/10.1016/j.gca.2018.04.024>
- Wharton, G., Arnell, N., Gregory, K., & Gurnell, A. (1989). River discharge estimated from channel dimensions. *Journal of Hydrology*, 106(3–4), 365–376. [https://doi.org/10.1016/0022-1694\(89\)90080-2](https://doi.org/10.1016/0022-1694(89)90080-2)